

Proteins. Author manuscript; available in PMC 2013 January 1.

Published in final edited form as:

Proteins. 2012 January; 80(1): 142–153. doi:10.1002/prot.23170.

# SIDEpro: a Novel Machine Learning Approach for the Fast and Accurate Prediction of Side-Chain Conformations

## Ken Nagata, Arlo Randall, and Pierre Baldi

Department of Computer Science and Institute for Genomics and Bioinformatics, University of California, Irvine

Ken Nagata: knagata@ics.uci.edu; Arlo Randall: arandall@ics.uci.edu; Pierre Baldi: pfbaldi@ics.uci.edu

#### Abstract

Accurate protein side-chain conformation prediction is crucial for protein modeling and existing methods for the task are widely used; however, faster and more accurate methods are still required. Here we present a new machine learning approach to the problem where an energy function for each rotamer in a structure is computed additively over pairs of contacting atoms. A family of 156 neural networks indexed by amino acid and contacting atom types is used to compute these rotamer energies as a function of atomic contact distances. Although direct energy targets are not available for training, the neural networks can still be optimized by converting the energies to probabilities and optimizing these probabilities using Markov Chain Monte Carlo methods. The resulting predictor SIDEpro makes predictions by initially setting the rotamer probabilities for each residue from a backbone dependent rotamer library, then iteratively updating these probabilities using the trained neural networks. After convergences of the probabilities, the side-chains are set to the highest probability rotamer. Finally, a post-processing clash reduction step is applied to the models. SIDEpro represents a significant improvement in speed and a modest, but statistically significant, improvement in accuracy when compared to the state-of-theart for rapid side-chain prediction method SCWRL4 on the following datasets: (1) 379 protein test set of SCWRL4; (2) 94 proteins from CASP9; (3) a set of 7 large protein-only complexes; and (4) a ribosome with and without the RNA. Using the SCWRL4 test set, SIDEpro's accuracy ( $\chi_1$ 86.14%,  $\chi_{1+2}$  74.15%) is slightly better than SCWRL4-FRM ( $\chi_1$  85.43%,  $\chi_{1+2}$  73.47%) and it is 7.0 times faster. On the same test set SIDEpro is clearly more accurate than SCWRL4-RRM ( $\chi_1$ 84.15%,  $\chi_{1+2}$  71.24%) and 2.4 times faster. Evaluation on the additional test sets yield similar accuracy results with SIDEpro being slightly more accurate than SCWRL4-FRM and clearly more accurate than SCWRL4-RRM; however, the gap in CPU time is much more significant when the methods are applied to large protein complexes. SIDEpro is part of the SCRATCH suite of predictors and available from: http://scratch.proteomics.ics.uci.edu/.

## 1 Introduction

Protein structure prediction is a fundamental problem in computational molecular biology and predicting the side-chain conformations for a given fixed backbone is an important subproblem [23]. Side-chain prediction methods are also critical for protein engineering, protein design, protein-protein docking [13, 1]. In both protein structure prediction and flexible protein-protein docking, the side-chain conformation predictions are relatively time intensive, and can be the limiting factor in how much search space can be explored. Thus, improvements in both speed and accuracy are highly desirable.

As a result, several methods have been proposed to address the side-chain prediction problem. SCWRL is one of the best methods and is widely used because it is generally fast and accurate, in addition it is convenient to download and run locally [5, 16]. SCWRL finds a combination of rotamers which minimizes an energy function based on rotamer probabilities and physical/chemical energy terms [5, 16]. There are two types rotamer libraries, backbone-independent and backbone-dependent. Backbone-independent rotamer libraries contain information on side-chain dihedral angles and rotamer populations. Backbone-dependent libraries contain the same information as a function of the backbone dihedral angles  $\phi$  and  $\psi$  [9, 10, 8, 7]. SCWRL, and most other successful prediction methods, utilize the probabilities from backbone-dependent rotamer libraries [5, 16] and some combination of physics-based energy terms based on electrotatics, hydrogen bonding, solvation free energy [11, 18], van der Waals forces or at least simple steric energy. In addition, many search methods have been applied to the side-chain prediction problem, such as dead-end elimination [12], Monte Carlo [17, 23, 11, 18], cyclical search [25, 26], selfconsistent mean field optimization [15, 20], integer programming [14], and graph decomposition [27, 16]. These methods rely on reducing the search space to pre-defined discrete sets of conformers for each side-chain (rigid rotamers) in order to make rapid predictions [1].

While physics-based energy functions have been applied with some success to the side-chain prediction problem in combination with discretized rigid rotamer models, they are not ideally suited for handling the coarseness of such models. In particular, repulsive physics-based energy terms are quite sensitive to slight changes in atom-atom distances. As a result, in the most accurate discretized models, some of the side-chains interactions inevitably have much higher repulsive energies relative to the native structures. In contrast, knowledge-based energy functions extracted from large training sets, which have been widely used in the field of protein structure prediction (e.g. [24, 28]), can be more tolerant to discretization. Furthermore, these knowledge-based energy functions can potentially capture subtle effects not captured by the physics-based approximations, and they can be trained directly on the most accurate discretized models.

Motivated by these issues, here we develop a new kind of knowledge-based energy function which is designed specifically for the rigid rotamer search space, and incorporate it into a novel side-chain prediction method, SIDEpro, which surpasses SCWRL4 in speed and accuracy. SIDEpro uses a family of artificial neural networks (ANNs) that are trained to compute an energy function based on atom-atom distances [2]. The structure models used to train the ANNs are modified versions of Protein Data Bank (PDB) structures [3], where each side-chain is independently set to the most accurate rigid rotamer. SIDEpro makes predictions by initially setting the probability of the rotamers for each residue using a backbone dependent rotamer library [9, 10, 8, 7]. Then it iteratively updates these rotamer probabilities using the ANNs energy until all the rotamer probabilities converge. Then, the side-chains are set to the rotamer with highest probability. Finally, a post-processing clash reduction procedure is applied to the models.

The remainder of the article is organized into sections covering the details of the SIDEpro methods, the results obtained for SIDEpro and SCWRL4 using several different benchmark datasets and metrics, and finally a short discussion section which summarizes the statistical significance of the results.

## 2 Methods

Here we present the details of the SIDEpro method in the following subsections: (1) the ANN architecture and energy function; (2) the training data and rotamer targets; (3) the full

probabilistic model; (4) the Markov Chain Monte Carlo optimization procedure; (5) the fast identification of atom contacts; (6) the elimination of rotamers with backbone clashes; (7) the prediction of rotamers; (8) the clash reduction procedure; and (9) the incorporation of fixed external atoms into the prediction method. A pseudocode outline of the prediction steps is also presented in Algorithm 1.

# 2.1 ANN Architecture and Energy Function

At its core, SIDEpro utilizes a family of neural networks to compute an energy function. This is a computational energy function and is not necessarily meant to represent a physical quantity. Each neural network is specialized to compute a particular term of the total energy associated with a particular amino acid and the distance between a particular pair of atom types. Thus, for instance, there is a neural network for Cysteine specialized for Sulphur-Carbon distances. While we did experiment with various ANN architectures, here we report the results obtained by using a simple three layer perceptron ANN architecture, for each member of the family (Figure 1). Each ANN receives a single external input, corresponding to a distance d between a pair of atoms of the given type, and produces a single output corresponding to the "energy" of the pair. The hidden layers typically have 15-20 units. The family comprises 156 different ANNs (Table 1), indexed by three variables corresponding to: (1) the amino acid type; (2) the atom type of the first atom in the pair, restricted to side chain atoms (no backbone atoms); and (3) the atom type of the second atom in the pair, including backbone atoms. The set of atom types is {N,C,O,S,H}. When the distance between two atoms is large enough they are not considered to be interacting in our model, thus we set the energy to zero when the distance, d, is greater than 7 Å. Thus the output e of a single network can be expressed as (Figure 1):

$$e = f(d; w) = \begin{cases} \sum_{h=1}^{H} w_{4h} \sigma(w_{2h} d + w_{1h}) + w_{31}, & d < 7 \\ 0, & \text{otherwise} \end{cases}$$
 (1)

where

w: ANN weights

 $\sigma$ : logistic sigmoid function ( $\sigma(x) = 1/(1 + e^{-x})$ )

H: number of hidden states (15-20)

Note that a sigmoid function is not applied to the output layer because the output is not restricted to [0,1].

By adding the contributions of each neural network applied to each pair of interacting atoms it is possible to compute the total energy of each rotamer, or the total energy of a protein. In particular, the energy of rotamer j for amino acid i is calculated as follows:

$$E_{ij} = \sum_{k=1}^{N_i} \sum_{l=1, l \neq i}^{L} \sum_{n=1}^{N_l} f_{a_i b_{ik} b_{ln}} (||X_{ijk} - X_{lr_{ln}}||; \mathbf{w})$$
(2)

where

 $E_{ij}$ : training energy for rotamer j at residue i

 $N_i$ : the number of atoms of residue i

L: the length of the amino acid sequence

 $X_{iik}$ : coordinate of k-th atom of rotamer j of residue i

 $a_i$ : amino acid type of residue i

 $b_{ik}$ : atom type of k-th atom of residue i

 $f_{aibikbln}(\cdot)$ : energy term computed by the ANN associated with the amino acid type of residue i, the atom type of the k-th atom of residue i, and the atom type of the n-th atom of residue l

 $r_i$ : rotamer target associated with residue i (see next section)

Here and in the rest of the paper we use bold-face fonts to denote vectors and contrast them with scalar variables.

A fundamental observation is that we do not have direct energy values that can be used to train the neural networks. However, we can derive rotamer targets from structures in the PDB [3]. As we shall see the energies computed by the ANNs can be converted into probabilities, and the ANNS can then be trained to maximize the probability of the target rotamers of the true structures. This optimization cannot be carried analytically but is implemented here using a Markov Chain Monte Carlo methods, essentially a variant of simulated annealing.

## 2.2 Training Data and Rotamer Targets

SIDEpro uses the publicly available backbone dependent rotamer library used by SCWRL3 [9][10][8][7][5] which was calculated from a set of 850 protein chains. The PISCES server was used to curate a diverse set of proteins to train the SIDEpro ANNs with the maximum mutual sequence identity set to 30%, maximum resolution of  $\leq 1.8$  Å, and a maximum R-factor of 20%. 2,661 proteins resulted from this search and 300 were randomly selected. Next, the 48 proteins with at least 25% sequence identity with one or protein in the SCWRL4 dataset were removed from the training set leaving 252 proteins for training.

Rather than using the raw PDB coordinates of these proteins, we set each side chain to the best matching rotamer in the corresponding rotamer library. Specifically, consider an amino acid i in a protein with  $R_i$  rotamers in the corresponding library. The library comes with a prior distribution  $p_{ij}$ ,  $j = 1,..., R_i$ . For each one of these rotamers, there is a vector of up to four angles  $\chi_{ij} = (\chi_{ij}^k)$ , k = 1,..., 4, with four corresponding normal distributions with known mean and standard deviations [7], so that:  $P(\chi_{ij}|\mu_{ij}, \sigma_{ij}) = \prod_{k=1}^{k=4} P(\chi_{ij}^k|\mu_{ij}^k, \sigma_{ij}^k)$ . Thus for a given amino acid i in a training protein in the PDB with observed angles  $\chi_i^{PDB}$ , we can use Bayes theorem to compute a posterior probability for each rotamer in the corresponding family in the form:

$$P(r_{ij}|\chi_i^{PDB}) = \frac{P(\chi_i^{PDB}|r_{ij})p_{ij}}{P(\chi_i^{PDB})}$$
(3)

Thus we assign a rotamer  $r_i$  to this amino acid by maximizing the posterior:

$$r_i = \underset{j}{\operatorname{argmax}} P(\chi_i^{PDB} | \mu_{ij}, \, \sigma_{ij}) p_{ij}$$
(4)

where  $\chi_i^{PDB}$  is the vector of  $\chi$  angles calculated from residue i in the native structure and  $p_{ij}$  is the probability of the j-th rotamer in the library for residue i.

## 2.3 Full Probabilistic Model

We can now proceed to use the energy computed by the ANNs to derive a full probabilistic model. The posterior probability of the training rotamer at residue i is the combination of the energy calculated by equation (2) when the weights of neural network w are given, with the rotamer library probability and is defined by:

$$P(r_i|w) = \frac{exp(-KE_{ir_i})p_{ir_i}}{\sum_{j=1}^{R_i} exp(-KE_{ij})p_{ij}}$$
(5)

where  $R_i$  is the number of rotamers for residue i and K is a constant (K = 0.1). We make the following standard independence approximation

$$P(r|w) = \prod_{i} (r_i|w) \tag{6}$$

This equation can be treated as a likelihood function with the posterior distribution of w given the data r provided by Bayes theorem:

$$P(w|r) = \prod_{i} \frac{P(r_i|w)P(w)}{P(r)}$$
(7)

Here P(w) is [ the weights w of the ANNs and P(r) is a normalizing constant that does not depend on w and can be ignored during the optimization process. Each ANN has its own prior distribution, which is modeled using a set of four independent zero-mean normal distributions in the form:

$$P(w|\alpha) = \prod_{i=1}^{4} \sqrt{\frac{\alpha_i}{2\pi}} \exp(-\frac{\alpha_i}{2} \sum_{j} w_{ij}^2)$$
(8)

where  $\alpha$  is a vector of hyper parameters, and each component  $\alpha_i$  controls the distribution of the corresponding weights [22, 19].

To complete the description of the full hierarchical probabilistic model, the positive hyperparameters  $\alpha_i$  can be assumed to be independent and follow a Gamma distribution

$$P(\alpha) = \prod_{i=1}^{4} \alpha_i^{k-1} \frac{\exp(-\alpha_i/\theta)}{\theta^k \Gamma(k)}$$
(9)

parameterized by k and  $\theta$ . After some experimentation, we fix the value of these parameters to k = 2 and  $\theta = 0.5$ .

## 2.4 Markov Chain Monte Carlo Optimization

To optimize the ANN weights, we use a Markov Chain Monte Carlo method [22], essentially a form of simulated annealing described, for instance, in [21]. More precisely, the idea is to use Gibbs sampling to sample from the posterior of  $\alpha$ , and Metropolis sampling to sample from the distribution of  $\mathbf{w}$ . By assuming  $\mathbf{r}$  and  $\alpha$  are independent, the posterior of  $\mathbf{w}$  for a single ANN can be written as:

$$P(w|r,\alpha) = \frac{P(w,r,\alpha)}{P(r,\alpha)} = \frac{P(r|w,\alpha)P(w|\alpha)P(\alpha)}{P(r)P(\alpha)} = \frac{P(r|w)P(w|\alpha)}{P(r)}$$
(10)

so that:

$$P(w|r,\alpha) \propto \left(\prod_{i=1}^{4} \sqrt{\frac{\alpha_i}{2\pi}}\right) \exp\left(-\sum_{i=1}^{4} \frac{\alpha_i}{2} \sum_{j} w_{ij}^2 + \sum_{i} \log P(r_i|w)\right)$$
(11)

Note that the last sum of Equation 11 ranges over all the amino acids in the training proteins where the corresponding ANN is used (e.g. for instance over all the cysteines in the set of training proteins). Similarly, for a single hyperparameter  $a_i$  associated with a specific ANN, we have

$$P(\alpha_i|r, w) = \frac{P(\alpha_i, r, w)}{P(r, w)} = \frac{P(r|w, \alpha_i)P(w|\alpha_i)P(\alpha_i)}{P(r, w)} = \frac{P(r|w)P(w|\alpha_i)P(\alpha_i)}{P(r, w)}$$
(12)

so that:

$$P(\alpha_{i}|r,w) \propto \alpha_{i}^{k-1} \exp\left(-\alpha_{i} \left(\theta^{-1} + \frac{1}{2} \sum_{j} w_{ij}^{2}\right)\right) \propto Gamma\left(k, \left(\theta^{-1} + \frac{1}{2} \sum_{j} w_{ij}^{2}\right)^{-1}\right)$$
(13)

Thus a Markov Chain Monte Carlo method is applied to get samples of the posterior distribution  $P(w, \alpha | r)$  by iteratively using:

- **1.** Gibbs sampling for  $\alpha^{(j)}$
- 2. Metropolis sampling for  $w^{(j)}$

Training proceeds by amino acid type, using all the ANNs associated with that particular amino acid type. For a given amino acid type and a given ANN, the learning algorithm

alternates between Gibbs sampling and Metropolis sampling. Thus at the *j*-iteration, we first get samples of  $\alpha^{(j+1)}$  by

$$\alpha_1^{(j+1)} \sim P(\alpha_1 | \alpha_2^{(j)}, \alpha_3^{(j)}, \alpha_4^{(j)}, w^{(j)})$$
 (14)

$$\alpha_2^{(j+1)} \sim P(\alpha_2 | \alpha_1^{(j+1)}, \alpha_3^{(j)}, \alpha_4^{(j)}, w^{(j)})$$
 (15)

$$\alpha_3^{(j+1)} \sim P(\alpha_3 | \alpha_1^{(j+1)}, \alpha_2^{(j+1)}, \alpha_4^{(j)}, w^{(j)})$$
 (16)

$$\alpha_4^{(j+1)} \sim P(\alpha_4 | \alpha_1^{(j+1)}, \alpha_2^{(j+1)}, \alpha_3^{(j+1)}, w^{(j)})$$
 (17)

Then we get a corresponding sample  $w^{(j+1)}$  by:

1. get candidate sample using

$$w^* \sim N(w^j, \sigma^2)$$
 (with  $\sigma^2 = 0.1$ ) (18)

2. accept sample  $w^*$  as  $w^{(j+1)}$  with probability  $\min \left[ \frac{P(w^*|r,\alpha^{(j+1)})}{P(w^{(j)}|r,\alpha^{(j+1)})}, 1 \right]$ , otherwise  $w^{(j+1)} = w^{(j)}$ 

The process is repeated for 500 iterations and the best observed weight  $w^*$  is saved and used in prediction. The number of iterations was chosen empirically based on prediction accuracy results obtained on the training set.

$$w^* = \underset{w^{(j)}}{\operatorname{argmax}} P(w^{(j)}|r, \alpha)$$
(19)

#### 2.5 Fast Identification of Atom Contacts

In principle, the previous approach could require looking at all pairs of atoms in a protein in order to compute the corresponding energy term. However, most pairs of atoms are separated by a distance greater than the 7 Å cutoff and therefore are considered as non-interacting. Thus, in order to significantly reduce the calculation costs, and associated CPU time, SIDEpro identifies the spatial neighbors of each residue and then ignores all non-neighbors in the energy calculations. The corresponding pruning is implemented using simple bounding boxes: if two bounding boxes do not intersect, then the corresponding pair of atoms is separated by more than 7.0 Å and can be ignored from the energy calculation.

Neighbors are defined by checking for overlap between boxes in 3D space which are determined by subsets of residue atoms. For each residue i, a box in 3D space is calculated for the backbone atoms  $(3Dbox_{BB}(i))$ , the side-chain atoms allowing all rotamers  $(3Dbox_{SC}(i))$ , and for each rotamer j  $(3Dbox_{Rot}(i,j))$ . Each box is defined as the space bound by six planes. For  $3Dbox_{BB}(i)$  the planes are:

$$x = \min_{k \in backbone(i)} X_{i1k_x} - 3.5 \tag{20}$$

$$x = \max_{k \in backbone(i)} X_{i1k_x} + 3.5 \tag{21}$$

$$y = \min_{k \in backbone(i)} X_{i1k_y} - 3.5$$
(22)

$$y = \max_{k \in backbone(i)} X_{i1k_y} + 3.5 \tag{23}$$

$$z = \min_{k \in backbone(i)} X_{i1k_z} - 3.5 \tag{24}$$

$$z = \max_{k \in backbone(i)} X_{i1k_z} + 3.5 \tag{25}$$

The planes which determine  $3Dbox_{SC}(i)$  are defined in the same manner, but the coordinates of all rotamers are searched:

$$x = \min_{j \in rotamers(i), k \in side-chain(i)} X_{ijk_x} - 3.5$$
(26)

$$x = \max_{j \in rotamers(i), k \in side-chain(i)} X_{ijk_x} + 3.5$$
(27)

$$y = \min_{j \in rotamers(i), k \in side-chain(i)} X_{ijk_y} - 3.5$$
(28)

$$y = \max_{j \in rotamers(i), k \in side-chain(i)} X_{ijk_y} + 3.5$$
(29)

$$z = \min_{j \in rotamers(i), k \in side-chain(i)} X_{ijk_z} - 3.5$$
(30)

$$z = \max_{j \in rotamers(i), k \in side-chain(i)} X_{ijk_z} + 3.5$$
(31)

The planes which determine  $3Dbox_{Rot}(i, j)$  are defined in the same manner, but using the side-chain atoms of a specific rotamer:

$$x = \min_{k \in side - chain(i)} X_{ijk_x} - 3.5 \tag{32}$$

$$x = \max_{k \in side - chain(i)} X_{ijk_x} + 3.5 \tag{33}$$

$$y = \min_{k \in side-chain(i)} X_{ijk_y} - 3.5 \tag{34}$$

$$y = \max_{k \in side-chain(i)} X_{ijk_y} + 3.5$$
(35)

$$z = \min_{k \in side - chain(i)} X_{ijk_z} - 3.5 \tag{36}$$

$$z = \max_{k \in side - chain(i)} X_{ijk_z} + 3.5 \tag{37}$$

Once the boxes are calculated, neighbor sets are defined for the backbone, side-chain, and each rotamer of each residue. The backbone neighbor set of residue i,  $Nbr_{BB}(i)$ , consists of all residues l such that  $3Dbox_{BB}(l)$  intersects  $3Dbox_{SC}(i)$ . The side-chain neighbor set,  $Nbr_{SC}(i)$ , consists of all residues l such that  $3Dbox_{SC}(l)$  intersects  $3Dbox_{SC}(i)$ . The rotamer neighbor set,  $Nbr_{Rot}(i,j)$ , consists of all rotamers l, m such that  $3Dbox_{Rot}(l,m)$  intersects  $3Dbox_{Rot}(i,j)$ . Note, however, that only the rotamers of residue-level neighbors need to be checked. This is a simple version of the approach used in SCWRL4 to construct bounding boxes for checking for clashes [16], but it is used here efficiently to avoid calculating distances for the vast majority of residue and atom pairs.

## 2.6 Elimination of Rotamers with Backbone Clashes

Once the residue neighbors are defined, the next step is to eliminate any rotamers which clash with the protein backbone. We define a rotamer's backbone clashing energy as:

$$E_{ij}^{VDW} = \sum_{k \in side-chain(i)l \in N} \sum_{br_{RR}(i)n \in backbone(l)} \begin{cases} (vdw_{ik} + vdw_{ln} - ||X_{ijk} - X_{l1n}||)^2, & \frac{||X_{ijk} - X_{l1n}||}{vdw_{ik} + vdw_{ln}} < 0.67 \\ 0, & \text{otherwise} \end{cases} < 0.67$$

(38)

where  $vdw_{ik}$  is the van der Waals radii of atom k of residue i. If  $E_i^{VDW} j > 1.0$  the rotamer is considered to be clashing with the backbone and it is excluded from the search. An

exception is made if all of the rotamers are clashing according to this criteria, in which case the least clashing rotamer (with lowest clashing energy) is used and all others are excluded. This approach reduces the search space significantly: on the SCWRL4 dataset approximately 20% of the rotamers are excluded from the search, resulting in a reduction of approximately 10% in average CPU time.

## 2.7 Prediction of Rotamers

After the rotamers which result in backbone clashes are excluded, the next step is to calculate the interaction energies between each rotamer of each residue and the entire backbone ( $E^{BB}$ ) and the side-chains of the previously defined neighboring residues ( $E^{SC}$ ). These interaction energies are calculated as:

$$E_{ij}^{BB} = \sum_{k \in side-chain(i) | \in Nbr_{BB}} \sum_{(i)n \in backbone(l)} f_{a_i b_{ik} b_{ln}} (||X_{ijk} - X_{l1n}||; w^*)$$
(39)

$$E_{ijlm}^{SC} = \sum_{k \in side-chain(i)n \in side-chain(l)} f_{a_ib_{ik}b_{ln}}(||X_{ijk} - X_{lmn}||; w^*)$$
(40)

where i and l represent amino acids, and j and m represent rotamers in the corresponding libraries. This decomposition is computationally efficient because the backbone is fixed and thus the backbone contribution  $E^{BB}$  is constant.

The probability estimates for each rotamer are initially set to the values from the rotamer library. Then, the structure-dependent energy values,  $E^{BB}$  and  $E^{SC}$ , are combined with the rotamer library probabilities to calculate the posterior probabilities for each rotamer. The

predicted energy of the individual rotamers ( $E_{ij}^P$ ) and the corresponding probability estimates ( $q_{ij}$ ) are the updated iteratively. Thus we first initialize the probability  $q_{ij}$  using the rotamer library default probabilities  $q_{ij} = p_{ij}$  and we then iterate the following two update equations:

$$E_{ij}^{P} = E_{ij}^{BB} + \sum_{l,m \in Nbr_{Rot}(i,j)} qlm E_{ijlm}^{SC}$$

$$\tag{41}$$

$$q_{ij} = \frac{exp(-KE_{ij}^{P})p_{ij}}{\sum_{k=1}^{R_{i}} exp(-KE_{ik}^{P})p_{ik}}$$
(42)

SIDEpro uses only 6 iterations of this procedure, which in general is sufficient for the values to converge and yield a predicted rotamer for each residue i by setting:  $\widehat{r_i} = \underset{j}{\operatorname{argmax}} q_{ij}$ .

Algorithm 1 SIDEpro Pseudocode.

Calculate boxes:  $3Dbox_{BB}$ ,  $3Dbox_{SC}$ , and  $3Dbox_{Rot}$ Calculate neighbor sets:  $Nbr_{BB}$ ,  $Nbr_{SC}$  and  $Nbr_{Rot}$ //set  $q_{ij}$  to be  $p_{ij}$  and remove clashing rotamers

```
for all residue i do
  for all rotamers at residue j do
      q_{ij}=p_{ij}
      E_{vdw}(i, j) = calculate equation (38)
      if E_{vdw}(i, j) > 1.0 then
         remove rotamer j
      end if
   end for
end for
//calculate E_{BB}
for all residue i do
  for all rotamers j at residue i do
      E_{BB}(i, j) = calculate equation (39)
  end for
end for
//calculate E_{SC}
for all residue i do
  for all rotamers j at residue i do
      for all l, m \in Nbr_{Rot}(i, j) do
         E_{SC}(i, j, l, m) = \text{calculate equation (40)}
      end for
  end for
end for
// update energies and probabilities until r converges
while any q_{ij} does not converge do
  for all residue i do
      //update energy of rotamers at residue i
      \mathbf{for} \; \mathbf{all} \; \mathrm{rotamers} \; j \; \mathrm{at} \; \mathrm{residue} \; i \; \mathbf{do}
         e_{ii} = calculate equation (41)
      end for
      //update probability of rotamers at residue i
      \mathbf{for} \; \mathbf{all} \; \mathrm{rotamers} \; j \; \mathrm{at} \; \mathrm{residue} \; i \; \mathbf{do}
         q_{ij} = calculate equation (42)
      end for
  end for
end while
for all residue i do
   \widehat{r_i} = \underset{j}{\operatorname{argmax}} q_{ij}
end for
where
       q_{ij}: updated probability of rotamer j at residue i
       p_{ij}: initial probability of rotamer j at residue i (from library)
       r: current set of rotamers i
```

 $\hat{r}_i$ : predicted rotamer for residue i

#### 2.8 Clash Reduction Procedure

The initial model produced by SIDEpro uses the means of the rotamer angles, thus it can be considered to be a rigid rotamer model. When a rigid rotamer model is used, some clashes are almost always observed in a compact protein model. In fact, the structures used for training contain some clashes because the rotamers were set to the mean of the closest rotamer in the library instead of using the raw coordinates. Since the SIDEpro energy function is a computational energy function learnt from data that contains some clashes, the initial model produced by SIDEpro may contain a certain number of steric clashes. To resolve these clashes we use a post-processing method which incorporates some flexibility into the rotamers.

The clashes are minimized using the following protocol. First, each residue is checked for clashes and for those with one or more clashing atoms, the  $\chi$  angles are updated to the mean  $(\mu) \pm$  the standard deviation  $(\sigma)$  multiplied by m (initially set to 0.5), then the distances between atoms are recalculated and the number of clashes are recounted. Next, the  $\chi$  angles are set such that the number of clashes is minimized among the combination of  $\mu \pm \sigma$ . This operation is repeated until the clash counts converge. When the clash counts converge, the value of m is increased to 1.0 and the process is repeated. When the clash counts converge, the value of m is again increased to 1.5 and the process is repeated for the final time. This method reduces the number of clashes without a noticeable effect on accuracy.

## 2.9 Incorporation of Fixed External Atoms into the Prediction Method

SIDEpro can optionally incorporate fixed atoms from external molecules (other proteins, RNA, DNA, ligands, etc.) into the prediction process. These external fixed atoms are handled in a manner similar to backbone atoms. SIDEpro builds boxes and neighbors for them, and calculates the energy  $E_{BB}$  as if the fixed atom were backbone atoms. Since the SIDEpro ANNs are trained only on C, O, N, H and S atoms, any other atoms types are simply treated as C. In addition to handling external molecules, a subset of side-chains in the protein being predicted can be treated as fixed. These are handled by ignoring the rotamers at the fixed positions and using the input coordinates for all calculations.

## 3 Results

#### 3.1 Evaluation Data and Protocol

To conduct a comparative evaluation of SIDEpro and SCWRL4, the following datasets are used: (1) the benchmark dataset of 379 proteins used to evaluate SCWRL4 [16] (SCWRL4 dataset); (2) 94 proteins determined by X-ray crystallography and released in the most recent Critical Assessment of Protein Structure Prediction Experiment (CASP9 dataset); (3) a small set of seven large protein complexes (pdb: 1RYP, 2JES, 2UVB, 3GND, 3GZU, 3K1F, 3KQK) ranging in size from 2760 to 8767 residues (COMPLEXES dataset); and (4) a ribosome (pdb: 1FJG) with and without the RNA (RIBOSOME dataset).

In SCWRL4 the default predictor utilizes a Flexibile Rotamer Model (FRM), but a Rigid Rotamer Model (RRM) is also available. The basic tradeoff between the two is that FRM is more accurate but slower than RRM [16]. Our preliminary tests of SCWRL4 confirmed this tradeoff, thus, both FRM and RRM are evaluated on each test dataset in this work and the summary results of both are compared to SIDEpro; however, only the FRM results are reported in the residue specific accuracy results for the SCWRL4 dataset (Table 3) and the CASP9 dataset (Table 5).

The summary results tables present the  $\chi_1$  accuracy,  $\chi_{1+2}$  accuracy, and RMSD averaged over all residues, the average CPU time per protein, and the total number of severe clashes and moderate clashes. The summary results are presented as follows: SCWRL4 dataset in Table 2, CASP9 dataset in Table 4, COMPLEXES dataset in Table 6, and the RIBOSOME dataset in Table 7. In all tables the best result according to each metric is shown in bold.

## 3.2 Accuracy

Accuracy is assessed using three standard metrics: (1) percentage of side-chains where  $\chi_1$  is within 40 degrees of the experimental structure angles; (2) percentage of side-chains with both  $\chi_1$  and  $\chi_2$  within 40°; and (3) root mean square deviation (RMSD), which is calculated using the absolute coordinates of the corresponding model and experimental structure side-chain atoms. For  $\chi_1$  evaluation, the symmetries of Phe and Tyr are accounted for by calculating  $\chi_1$  using both symmetric atoms and checking each result versus the experimental structure. For  $\chi_{1+2}$  evaluation the symmetries of Asp, Phe, and Tyr are accounted for similarly. In evaluating the RMSD the symmetries of Arg, Asp, Glu, Phe, and Tyr are accounted for by calculating the RMSD using both possible atom mappings and keeping the minimum result.

The accuracy summaries calculated on the SCWRL4 dataset are presented in Table 2. Overall, SIDEpro is slightly more accurate than SCWRL4-FRM according to all three accuracy measures:  $\chi_1$  (86.14% vs 85.43%),  $\chi_{1+2}$  (74.15% vs 73.47%), and RMSD (0.911 Å vs 0.948 Å). SCWRL4-RRM is the least accurate according to all three measures. Table 3 provides the residue specific accuracy results of SIDEpro and SCWRL4-FRM on the SCWRL4 dataset [16].

The accuracy summaries calculated on the CASP9 dataset are presented in Table 4. Again, SIDEpro is slightly more accurate than SCWRL4-FRM according to all three accuracy measures:  $\chi_1$  (85.01% vs 84.21%),  $\chi_{1+2}$  (72.76% vs 72.21%), and RMSD (0.940 Å vs 0.977 Å). Again, SCWRL4-RRM is least accurate according to all three measures. Table 5 provides the residue specific accuracy results of SIDEpro and SCWRL4-FRM on for the CASP9 dataset.

The accuracy summaries calculated on the COMPLEXES dataset are presented in Table 6. On this set SIDEpro is clearly more accurate than SCWRL4-FRM according to all three accuracy measures:  $\chi_1$  (79.73% vs 77.99%),  $\chi_{1+2}$  (64.19% vs 62.57%), and RMSD (1.109 Å vs 1.184 Å). Again, SCWRL4-RRM is least accurate according to all three measures.

The accuracy summaries calculated on the RIBOSOME dataset with and without RNA are presented in Table 7. When the predictions are made without the RNA coordinates provided to the methods SIDEpro is more accurate than SCWRL4-FRM according to all three accuracy measures:  $\chi_1$  (71.50% vs 70.61%),  $\chi_{1+2}$  (53.60% vs 52.37%), and RMSD (1.504 Å vs 1.559 Å). SCWRL4-RRM is the least accurate according to all three measures. When the predictions are made in the presence of the RNA coordinates the accuracies of all three methods improve according to all three measures. SIDEpro is still the most accurate, followed by SCWRL4-FRM, with results of  $\chi_1$  (74.30% vs 72.31%),  $\chi_{1+2}$  (56.00% vs 54.49%), and RMSD (1.423 Å vs 1.480 Å). SCWRL4-RRM is still the least accurate according to the three measures.

## 3.3 CPU Time

Figure 2 shows the relationship between the number of residues in a protein and the prediction time for SIDEpro, SCWRL4-FRM, and SCWRL4-RRM using the 379 proteins from the SCWRL4 dataset. For SIDEpro, the time follows a predictable linear increase according to the number of residues with a Pearson correlation of 0.97. For both SCWRL

methods, the time generally increases with the number of residues, but the relationship is much less predictable. The Pearson correlation for SCWRL4-RRM is 0.53 and for SCWRL4-RRM it is 0.48. On the SCWRL4 dataset the average CPU time needed by each method to make prediction is 1.61s for SIDEpro, 11.09s for SCWRL4-FRM, and 3.84s for SCWRL4-RRM (Table 2). The gap in CPU time between SIDEpro and SCWRL is more significant on the CASP9 dataset where the average CPU times are 2.06s for SIDEpro, 19.06s for SCWRL4-FRM, and 10.64s for SCWRL4-RRM (Table 4). For both of these datasets the times are calculated using all protein chains in each PDB file as input. The CPU times for all experiments are obtained using an AMD Turion 64 ×2 Mobile Technology TL-60+ at 2.00 GHz, with 3.00 GB of RAM, and running 32-bit Microsoft Windows Vista Home Premium Service Pack 2.

For the COMPLEXES dataset the gap between the CPU times required by the different methods is much more significant. The average CPU times are 26.9s for SIDEpro, 583.9s for SCWRL4-FRM, and 409.4s for SCWRL4-FRM (Table 6). For this dataset the times are calculated using the biological assemblies as input.

On the RIBOSOME dataset without the RNA the CPU times are 11.8s for SIDEpro, 180.0s for SCWRL4-FRM, and 102.1s for SCWRL4-RRM. When the RNA coordinates are provided the CPU time for SIDEpro increases only slightly to 13.7s; in contrast the time jumps to 4020.7s for SCWRL4-FRM and 796.2s for SCWRL4-RRM (Table 7). Note that all three methods exhibit similar increases in accuracy when the RNA coordinates are utilized in prediction. In sum, once trained, SIDEpro is significantly faster than the other programs.

#### 3.4 Clash Assessment

Two types of clashes are defined here and used for assessment: severe and moderate. In order to assess the frequency of clashes appropriately and to make fair comparisons we utilized SCWRL parameters related to steric repulsion to define clashes.

The SCWRL repulsive energy term applies no penalty if the observed distance, d, between atoms i and j is greater than the sum of their hard sphere radii  $(vdw_{ij})$ . The maximum penalty is applied if  $d/vdw_{ij} < .8325$ , and a linear ramp is used if  $.8235 \le d/vdw_{ij} \le 1$  [4, 5, 16]. Thus, we define a moderate clash to occur if  $.8235 \le d/vdw_{ij} \le 1$ , and a severe clash if  $d/vdw_{ij} < .8325$ . Clashes are counted at the level of residue pairs and only the minimum observed  $d/vdw_{ij}$  for each residue pair is considered. This means that each residue pair can only be counted as one of: (1) unclashed, (2) moderate clash, or (3) severe clash. The radii used in this assessment are the same as those used in the SCWRL steric energy: carbon, 1.6 Å; oxygen, 1.3 Å; nitrogen, 1.3 Å; and sulfur 1.7 Å.

The counts of severe and moderate clashes observed in the models produced by SIDEpro, SCWRL4-FRM, and SCWRL4-RRM are presented in the summary tables for each dataset. The clashes observed in the corresponding PDB structures are also included for comparison. In general, the disparity in the number of clashes between the PDB structures and the models produced by all methods demonstrates that there is still room for improvement in terms of clash resolution.

On the SCWRL4 dataset the SIDEpro models have fewer severe clashes (305 vs 1047) and fewer moderate clashes (7227 vs 9743) than SCWRL4-FRM models, and also fewer severe clashes than SCWRL4-RRM models (496); however, SCWRL4-RRM has the smallest number of moderate clashes (6661).

On the CASP9 dataset the pattern is repeated. SIDEpro models have fewer severe clashes (112 vs 356) and fewer moderate clashes (2403 vs 3170) than SCWRL4-FRM models, and

also fewer severe clashes than SCWRL4-RRM models (172); however, SCWRL4-RRM has the smallest number of moderate clashes (2117).

On the COMPLEXES dataset the pattern is repeated again. SIDEpro models have fewer severe clashes (253 vs 972) and fewer moderate clashes (6114 vs 7493) than SCWRL4-FRM models, and also fewer severe clashes than SCWRL4-RRM models (540); however, SCWRL4-RRM has the smallest number of moderate clashes (5490). This same pattern is also repeated on the RIBOSOME dataset both with and without RNA.

#### 4 Discussion

Methods that can predict protein side-chains quickly and accurately can be applied in many important applications in computational molecular biology. In this investigation, we have described a new machine learning approach to the problem, resulting in a new predictor SIDEpro, and compared its performance to SCWRL4 on various datasets. In all cases, we found the same basic result: SIDEpro is more accurate and faster than both versions of SCWRL4. Table 8 summarizes the statistical significance of SIDEpro's improvements in accuracy, with respect to SCWRL4-FRM and SCWRL4-RRM, for each dataset using each metric. Considering the results on the large datasets, SCWRL4, CASP9, and COMPLEXES, the difference between SIDEpro and SCWRL4-FRM accuracies is significant at p<0.001 for all results except CASP9  $\chi_{1+2}$  where p=0.05. When comparing SIDEpro and SCWRL4-RRM on the large datasets, all of the accuracy results presented are significant at p<1.0e-10.

When compared to the SCWRL4 Free Rotamer Model SIDEpro represents a moderate, but statistically significant improvement in accuracy, but the difference in CPU time is significant: SIDEpro is from 7 to 20 times faster depending on the dataset. When compared to the SCWRL4 Rigid Rotamer Model the improvement in accuracy is more significant, and SIDEpro is still from 2 to 15 times faster. In addition, SIDEpro handles proteins complexed with non-protein molecules robustly, with only a moderate increase in CPU time. Thus, SIDEpro is a useful new tool for the prediction of protein side-chains in both low- and high-throughput research projects. SIDEpro is freely available for academic use as part of the SCRATCH suite [6] available at http://scratch.proteomics.ics.uci.edu/ both as a web server and as downloadable code.

# **Acknowledgments**

Work partly supported by NIH Biomedical Informatics Training grant (LM-07443-01), NSF MRI grant (EIA-0321390), and NSF grants IIS-0513376 to PB, NIH/NLM Pathwayto Independence Award (K99LM010821) to AR, and by the UCI Institute for Genomics and Bioinformatics.

## References

- Andrusier, Nelly; Mashiach, Efrat; Nussinov, Ruth; Wolfson, Haim J. Principles of flexible proteinprotein docking. Proteins: Structure, Function, and Bioinformatics. 2008; 73(2):271–289.
- 2. Baldi, Pierre; Brunak, Soren. Bioinformatics: the machine learning approach. MIT Press; 2001.
- 3. Berman HM, Battistuz T, Bhat TN, Bluhm WF, Bourne PE, Burkhardt K, Feng Z, Gilliland GL, Iype L, Jain S, Fagan P, Marvin J, Padilla D, Ravichandran V, Schneider B, Thanki N, Weissig H, Westbrook JD, Zardecki C. The protein data bank. Acta Crystallographica, Section D: Biological Crystallography. 2002; 58:899–907.
- Bower MJ, Cohen FE, Dunbrack RL Jr. Prediction of protein side-chain rotamers from a backbonedependent rotamer library: A new homology modeling tool. J Mol Biol. 1997; 267:1268–1282. [PubMed: 9150411]
- Canutescu AA, Shelenkov AA, Dunbrack RL Jr. A graph-theory algorithm for rapid protein sidechain prediction. Protein Sci. sep; 2003 12(9):2001–2004. [PubMed: 12930999]

 Cheng J, Randall AZ, Sweredoski MJ, Baldi P. Scratch: a protein structure and structural feature prediction server. Nucleic Acids Res. 2005; 33:W72–76. [PubMed: 15980571]

- 7. Dunbrack RL Jr. Rotamer libraries in the 21st century. Curr Opin Struct Biol. 2002; 12:431–440. [PubMed: 12163064]
- 8. Dunbrack RL Jr, Cohen FE. Bayesian statistical analysis of protein sidechain rotamer preferences. Protein Sci. 1997; 6:1661–1681. [PubMed: 9260279]
- Dunbrack RL Jr, Karplus M. Backbone-dependent rotamer library for proteins: Application to sidechain prediction. J Mol Biol. 1993; 230:543–574. [PubMed: 8464064]
- Dunbrack RL Jr, Karplus M. Conformational analysis of the backbone-dependent rotamer preferences of protein sidechains. Nat Struct Biol. 1994; 1:334

  –340. [PubMed: 7664040]
- 11. Eyal, Eran; Najmanovich, Rafael; Mcconkey, Brendan J.; Edelman, Marvin; Sobolev, Vladimir. Importance of solvent accessibility and contact surfaces in modeling side-chain conformations in proteins. Journal of Computational Chemistry. 2004; 25(5):712–724. [PubMed: 14978714]
- 12. Goldstein RF. Efficient rotamer elimination applied to protein side-chains and related spin glasses. Biophys J. 1994; 66:1335–1340. [PubMed: 8061189]
- Gray, Jeffrey J.; Moughon, Stewart; Wang, Chu; Schueler-Furman, Ora; Kuhlman, Brian; Rohl, Carol A.; Baker, David. Protein-protein docking with simultaneous optimization of rigid-body displacement and side-chain conformations. Journal of Molecular Biology. 2003; 331(1):281–299. [PubMed: 12875852]
- 14. Kingsford CL, Chazelle B, Singh M. Solving and analyzing side-chain positioning problems using linear and integer programming. Bioinformatics. 2005; 21:1028–1036. [PubMed: 15546935]
- Koehl P, Delarue M. Application of a self-consistent mean field theory to predict protein sidechains conformation and estimate their conformational entropy. J Mol Biol. 1994; 239:249–275.
   [PubMed: 8196057]
- Krivov GG, Shapovalov MV, Dunbrack RL Jr. Improved prediction of protein side-chain conformations with scwrl4. Protein. dec; 2009 77(4):778–95.
- 17. Liang S, Grishin NV. Side-chain modeling with an optimized scoring function. Protein Sci. 2002; 11:322–331. [PubMed: 11790842]
- 18. Lu, Mingyang; Dousis, Athanasios D.; Ma, Jianpeng. Opus-rota: A fast and accurate method for side-chain modeling. Protein Science. 2008; 17(9):1576–1585. [PubMed: 18556476]
- 19. MacKay, DJC. ASHRAE Transactions. Vol. 100. ASHRAE; 1994. Bayesian non-linear modelling for the prediction competition; p. 1053-1062.
- 20. Mendes, Joaquim; Soares, Čiaaudio M.; Carrondo, Maria Armil'nia. Improvement of side-chain modeling in proteins with the self-consistent mean field theory method based on an analysis of the factors influencing prediction. Biopolymers. 1999; 50(2):111–131. [PubMed: 10380336]
- 21. Muramatsu D, Kondo M, Sasaki M, Tachibana S, Matsumoto T. A markov chain monte carlo algorithm for bayesian dynamic signature verification. IEEE T Inf Foren Sec. 2006; 1:22–34.
- 22. Neal, RM. Bayesian Learning for Neural Networks. Springer-Verlag; 1996.
- 23. Rohl, Carol A.; Strauss, Charlie EM.; Chivian, D.; Baker, D. Modeling structurally variable regions in homologous proteins with rosetta. Proteins. 2004; 55:656–677. [PubMed: 15103629]
- 24. Simons K, Ruczinski I, Kooperberg C, Fox BA, Bystroff C, Baker D. Improved recognition of native-like protein structures using a combination of sequence-dependent and sequence-independent features of proteins. Proteins. 1999; 34:82–95. [PubMed: 10336385]
- 25. Xiang Z, Honig B. Extending the accuracy limits of prediction for side-chain conformations. J Mol Biol. 2001; 311:421–430. [PubMed: 11478870]
- 26. Xiang, Zhexin; Steinbach, Peter J.; Jacobson, Matthew P.; Friesner, Richard A.; Honig, Barry. Prediction of side-chain conformations on protein surfaces. Proteins: Structure, Function, and Bioinformatics. 2007; 66(4):814–823.
- 27. Xu, Jinbo. Rapid protein side-chain packing via tree decomposition. In: Miyano, Satoru; Mesirov, Jill; Kasif, Simon; Istrail, Sorin; Pevzner, Pavel; Waterman, Michael, editors. Research in Computational Molecular Biology, volume 3500 of Lecture Notes in Computer Science. Springer; Berlin/Heidelberg: 2005. p. 423-439.

28. Zhang Y, Kolinski A, Skolnick J. Touchstone:ii a new approach to ab initio protein structure prediction. Biophys J. 2003; 85:1145–1164. [PubMed: 12885659]

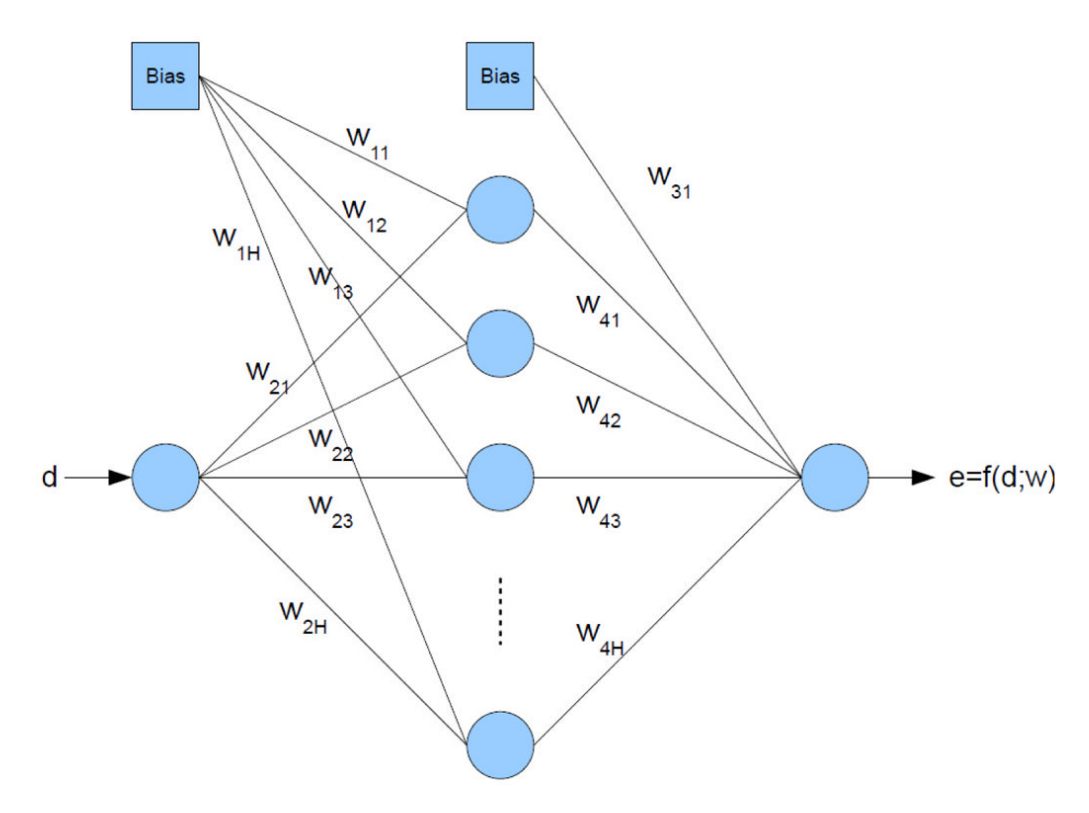


**Figure 1.** Network Architecture

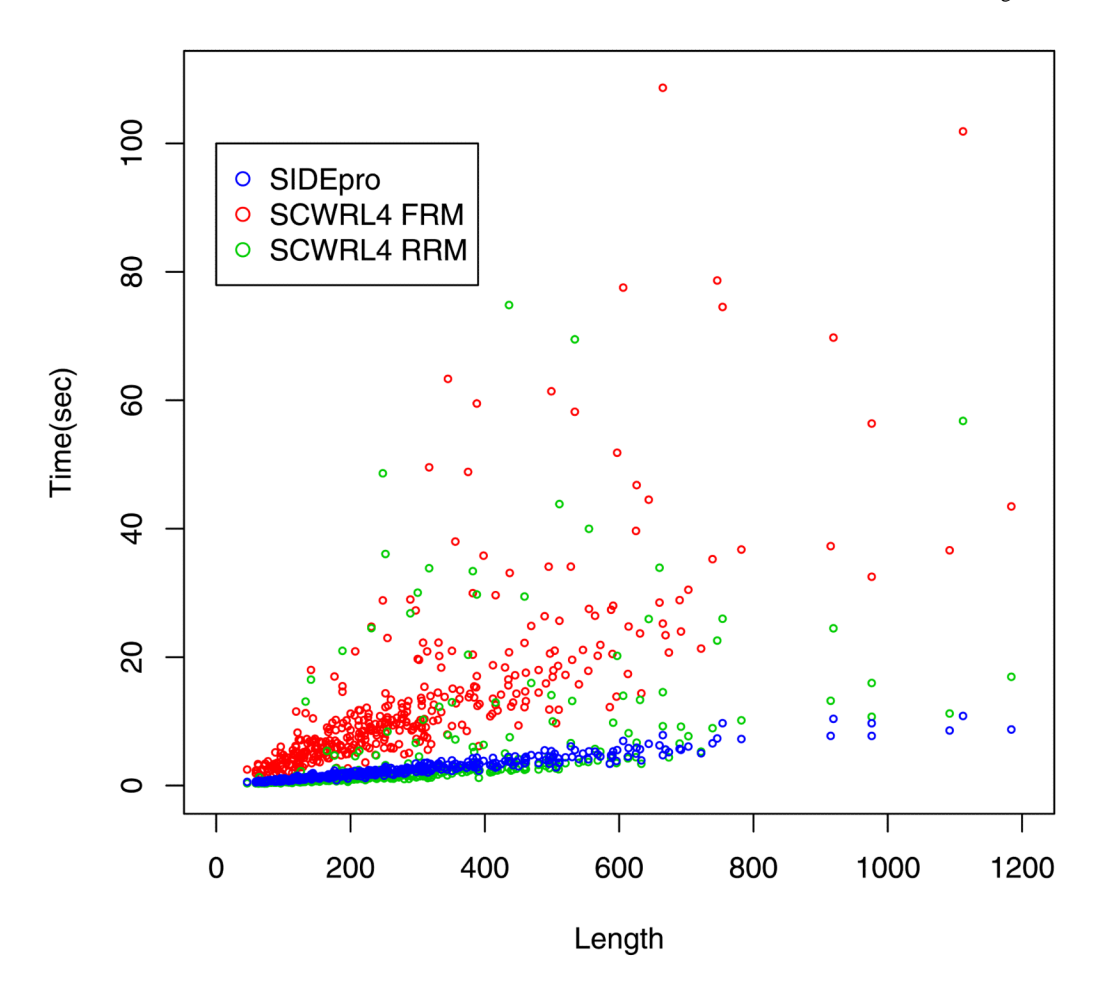


**Figure 2.**CPU Times versus Protein Length for the 379 Protein SCWRL4 Dataset. The CPU time required by SIDEpro increases linearly with the number of residues, with a Pearson correlation of 0.97. For both SCWRL methods, the CPU time generally increases with the number of residues, but the relationships are less predictable. The Pearson correlation for SCWRL4-FRM is 0.53 and for SCWRL4-RRM it is 0.48.

## Table 1

The number of ANNs for each amino acid. Note that ALA and GLY are excluded because no side-chain search is needed for these residues. For CYS, we use two different ANNs for Sulphur-Sulphur interactions corresponding to S-S(CYS) and S-S(MET).

| Amino Acid | Number of ANNs |
|------------|----------------|
| CYS        | 6              |
| ASP        | 10             |
| GLU        | 10             |
| PHE        | 5              |
| HIS        | 10             |
| ILE        | 5              |
| LYS        | 10             |
| LEU        | 5              |
| MET        | 10             |
| ASN        | 15             |
| PRO        | 5              |
| GLN        | 15             |
| ARG        | 10             |
| SER        | 5              |
| THR        | 10             |
| VAL        | 5              |
| TRP        | 10             |
| TYR        | 10             |
| Total      | 156            |

Table 2 SCWRL4 Dataset Summary Results: 379 Proteins, 58229 Residues

| Method     | (%)   | χ <sub>1+2</sub> (%) | RMSD (Å) | Time (s) | RMSD (Å) Time (s) Severe Clashes | Moderate Clashes |
|------------|-------|----------------------|----------|----------|----------------------------------|------------------|
| PDB        |       |                      |          |          | 31                               | 2048             |
| SIDEpro    | 86.14 | 74.15                | 0.911    | 1.61     | 305                              | 7227             |
| SCWRL4-FRM | 85.43 | 73.47                | 0.948    | 11.09    | 1047                             | 9743             |
| SCWRL4-RRM | 84.15 | 71.24                | 0.995    | 3.84     | 496                              | 6661             |

Table 3

SCWRL4 Dataset Residue Specific Accuracy Results

| A A Tymo | June J   | , 1 <u>7</u> | χ <sub>1</sub> (%) | χ1+2    | χ <sub>1+2</sub> (%) | RMS     | RMSD (Å) |
|----------|----------|--------------|--------------------|---------|----------------------|---------|----------|
| AA Lype  | AA COUNT | SIDEpro      | SCWRL4             | SIDEpro | SCWRL4               | SIDEpro | SCWRL4   |
| ARG      | 3636     | 78.8         | 78.3               | 65.2    | 6.99                 | 2.24    | 2.33     |
| ASN      | 2883     | 85.4         | 83.9               | 61.6    | 59.5                 | 1.04    | 1.09     |
| ASP      | 4018     | 84.8         | 84.0               | 75.3    | 75.4                 | 0.81    | 0.82     |
| CYS      | 1001     | 90.4         | 90.3               |         |                      | 0.48    | 0.47     |
| GLN      | 2512     | 79.1         | 78.7               | 6.09    | 58.9                 | 1.64    | 1.69     |
| GLU      | 4644     | 73.2         | 72.8               | 9.75    | 56.2                 | 1.47    | 1.50     |
| HIS      | 1543     | 9.68         | 6.78               | 53.4    | 50.7                 | 1.27    | 1.35     |
| ILE      | 3968     | 92.6         | 0.96               | 83.4    | 84.7                 | 0.45    | 0.43     |
| LEU      | 6558     | 93.5         | 92.1               | 86.5    | 86.2                 | 0.56    | 0.58     |
| LYS      | 3901     | 79.3         | 6.97               | 66.5    | 63.3                 | 1.63    | 1.73     |
| MET      | 1410     | 83.8         | 83.8               | 74.5    | 70.3                 | 1.14    | 1.27     |
| PHE      | 2717     | 7.56         | 95.3               | 92.7    | 92.6                 | 9.65    | 0.72     |
| PRO      | 3233     | 83.7         | 85.5               | 80.2    | 81.6                 | 0.27    | 0.26     |
| SER      | 4107     | 74.0         | 70.8               |         |                      | 0.73    | 0.80     |
| THR      | 3790     | 8.06         | 5.06               |         |                      | 0.39    | 0.39     |
| TRP      | 626      | 91.6         | 92.1               | 82.6    | 79.5                 | 1.16    | 1.37     |
| TYR      | 2346     | 94.5         | 94.7               | 91.0    | 92.1                 | 0.83    | 98.0     |
| VAL      | 5019     | 93.2         | 93.1               |         |                      | 0.32    | 0.32     |
| Combined | 58265    | 86.14        | 85.43              | 74.15   | 73.47                | 0.911   | 0.948    |

Table 4 CASP9 Dataset Summary Results: 94 Proteins, 17885 Residues

| Method     | χ1(%) | $\chi_{1+2}(\%)$ | RMSD (Å) | Time (s) | Severe Clashes | $\chi_1(\%)$ $\chi_{1+2}(\%)$ RMSD (Å) Time (s) Severe Clashes Moderate Clashes |
|------------|-------|------------------|----------|----------|----------------|---|
| PDB        |       |                  |          |          | 7              | 620   |
| SIDEpro    | 85.01 | 72.76            | 0.940    | 2.06     | 112            | 2403  |
| SCWRL4-FRM | 84.21 | 72.21            | 0.977    | 19.06    | 356            | 3170  |
| SCWRL4-RRM | 82.83 | 66.79            | 1.030    | 10.64    | 172            | 2117  |

CASP9 Dataset Residue Specific Accuracy Results

Table 5

|          |          | χ1(     | χ <sub>1</sub> (%) | χ1+;    | χ <sub>1+2</sub> (%) | RMS     | RMSD (Å) |
|----------|----------|---------|--------------------|---------|----------------------|---------|----------|
| AA 1ype  | AA Count | SIDEpro | SCWRL4             | SIDEpro | SCWRL4               | SIDEpro | SCWRL4   |
| ARG      | 1118     | 78.2    | 78.8               | 64.3    | 66.2                 | 2.19    | 2.24     |
| ASN      | 901      | 86.0    | 83.0               | 63.3    | 58.0                 | 96.0    | 1.07     |
| ASP      | 1396     | 85.9    | 85.5               | 73.1    | 73.6                 | 0.81    | 0.81     |
| CYS      | 249      | 89.2    | 8.06               |         |                      | 0.52    | 0.48     |
| GLN      | 756      | 82.7    | 80.0               | 65.5    | 60.3                 | 1.51    | 1.64     |
| OLU      | 1488     | 69.3    | 69.2               | 55.4    | 54.4                 | 1.51    | 1.53     |
| HIS      | 548      | 86.3    | 87.0               | 53.3    | 54.9                 | 1.34    | 1.31     |
| ILE      | 1341     | 94.6    | 94.6               | 9.62    | 81.4                 | 0.53    | 0.51     |
| LEU      | 2064     | 92.0    | 90.1               | 83.9    | 82.7                 | 0.63    | 0.67     |
| LYS      | 1172     | 78.6    | 6.77               | 64.9    | 63.7                 | 1.61    | 1.66     |
| MET      | 72       | 79.2    | 77.8               | 76.4    | 68.1                 | 1.06    | 1.20     |
| PHE      | 998      | 92.6    | 94.2               | 91.3    | 91.2                 | 0.67    | 0.77     |
| PRO      | 931      | 83.9    | 8.98               | 75.4    | 77.8                 | 0.30    | 0.28     |
| SER      | 1340     | 72.6    | 9.89               |         |                      | 0.77    | 0.85     |
| THR      | 1105     | 87.4    | 86.2               |         |                      | 0.48    | 0.50     |
| TRP      | 302      | 92.4    | 92.1               | 82.5    | 76.8                 | 1.18    | 1.42     |
| TYR      | 821      | 94.3    | 93.8               | 7:06    | 91.4                 | 98.0    | 0.91     |
| VAL      | 1415     | 89.0    | 89.1               |         |                      | 0.44    | 0.43     |
| Combined | 17885    | 85.01   | 84.21              | 72.76   | 72.21                | 0.940   | 726.0    |

Table 6 COMPLEXES Dataset Summary Results: 7 Protein Complexes with 91 Chains, 30734 Residues

| Method     | χ1(%) | $\chi_{1+2}(\%)$ | RMSD (Å) | Time (s) | Severe Clashes | χ <sub>1+2</sub> (%) RMSD (Å) Time (s) Severe Clashes Moderate Clashes |
|------------|-------|------------------|----------|----------|----------------|--|
| PDB        |       |                  |          |          | 37             | 2349   |
| SIDEpro    | 79.73 | 64.19            | 1.109    | 26.9     | 253            | 6114   |
| SCWRL4-FRM | 77.99 | 62.57            | 1.184    | 583.9    | 972            | 7493   |
| SCWRL4-RRM | 76.87 | 59.87            | 1.237    | 409.4    | 540            | 5490   |

Table 7 RIBOSOME Dataset Summary Results: 21 Protein Chains, 2001 Residues

| Method      | $\chi_1(\%)$ | $\chi_{1+2}(\%)$ | RMSD (Å) | Time (s) | Severe Clashes | $\chi_1(\%)$ $\chi_{1+2}(\%)$ RMSD $(\mathring{A})$ Time $(s)$ Severe Clashes Moderate Clashes |
|-------------|--------------|------------------|----------|----------|----------------|--|
| Without RNA |              |                  |          |          |                |  |
| PDB         |              |                  |          |          | 0              | 370  |
| SIDEpro     | 71.50        | 53.60            | 1.504    | 11.8     | 13             | 386  |
| SCWRL4-FRM  | 70.61        | 52.37            | 1.559    | 180.0    | 54             | 433  |
| SCWRL4-RRM  | 69.57        | 50.31            | 1.607    | 102.1    | 32             | 309  |
| With RNA    |              |                  |          |          |                |  |
| SIDEpro     | 74.30        | 56.00            | 1.423    | 13.7     | 14             | 371  |
| SCWRL4-FRM  | 72.31        | 54.49            | 1.480    | 4020.7   | 65             | 477  |
| SCWRL4-RRM  | 71.46        | 52.81            | 1.524    | 796.2    | 39             | 340  |

 $\label{thm:continuous} \begin{tabular}{ll} Table 8 \\ Statistical Significance (p-values) of SIDE pro Improvement with Respect to SCWRL4. \\ Results significant at p<0.001 are shown in bold \\ \end{tabular}$ 

| Dataset                | AA Count | χ1       | X1+2     | RMSD     |
|------------------------|----------|----------|----------|----------|
| SIDEpro wrt SCWRL4-FRM |          |          |          |          |
| SCWRL4                 | 58265    | 3.1e-08  | 9.8e-05  | <1.0e-10 |
| CASP9                  | 17885    | 7.1e-04  | 5.1e-02  | 3.4e-08  |
| COMPLEXES              | 30734    | <1.0e-10 | 1.5e-09  | <1.0e-10 |
| RIBOSOME               | 2001     | 1.7e-01  | 1.4e-01  | 1.4e-02  |
| RIBOSOME + rna         | 2001     | 1.5e-02  | 9.3e-02  | 1.4e-02  |
| SIDEpro wrt SCWRL4-RRM |          |          |          |          |
| SCWRL4                 | 58265    | <1.0e-10 | <1.0e-10 | <1.0e-10 |
| CASP9                  | 17885    | <1.0e-10 | <1.0e-10 | <1.0e-10 |
| COMPLEXES              | 30734    | <1.0e-10 | <1.0e-10 | <1.0e-10 |
| RIBOSOME               | 2001     | 2.1e-02  | 2.2e-03  | 2.1e-05  |
| RIBOSOME + rna         | 2001     | 1.3e-03  | 3.1e-03  | 4.1e-05  |